Journal of Physics: Conference Series **73** (2007) 012008 doi:10.1088/1742-6596/73/1/012008

Magnetic tomography for fuel cells - current status and problems

Karl-Heinz Hauer and Roland Potthast[1]

TomoScience GbR, Major-Hirst-Str. 11 (Innovationscampus), D-38442 Wolfsburg, Tel.: 05361/897-7300, Fax.: 05361/897-1060
Department of Mathematics, University of Reading, Whiteknights, PO Box 220, Berkshire, RG6 6AX, UK.

E-mail: [1]r.w.e.potthast@reading.ac.uk

Abstract. We provide a survey about the status and open problems for magnetic tomography for fuel cells. A number of papers are reviewed which develop the subject including theory of simulation and inversion, uniqueness questions, reconstruction algorithms and real data applications. In particular, this work describes a number of yet unpublished results and experiments. Our goal is to provide a complete picture of the status-quo of magnetic tomography for fuel cells which includes the recent scientific and engineering results as well as an introduction into open questions and upcoming developments. We believe that magnetic tomography as an ill-posed and non-unique inverse source problem reflects key problems of many applied inverse problems. In particular, the challenges of real data applications reflect the challenges of the area of inverse problems as a whole and provide inside into generic problems of this important area of applied mathematics.

1. Introduction

Magnetic tomography is concerned with the reconstruction of currents from their magnetic fields. Current reconstructions are of importance for several practical applications. In medicine the magnetic fields around the brain reflect the neural activity in different areas of the animal or human being. The location of source distributions is important for planning of surgery and as a general means of diagnosis. Industrial applications use magnetic fields in such diverse areas as steal production and fuel cells. For the fuel cell application the reconstruction of current densities is needed for the development, monitoring and testing of the chemical and physical processes in fuel cells.

The basic setting of *magnetic tomography for fuel cells* has been pioneered in a series of papers [10] on *numerical simulations* with the Tikhonov regularization for reconstruction, [11] on the underlying *anisotropic forward problem* via the finite integration technique, [5] on the *uniqueness question* for current reconstructions in full stacks and [6] on the full applied *measurement method* including the design of a machine for such measurements. In contrast to the medical applications, the currents in fuel cells do *not have internal sources*. This leads to an underlying partial differential equations without source terms on the right-hand side. It strongly influences the uniqueness results and reconstruction techniques.

Fuel cells are chemical devices which transform chemical energy into electrical energy. The basic principle for a hydrogen-oxygen fuel cell is shown in Figure 1. At the anode (+) hydrogen

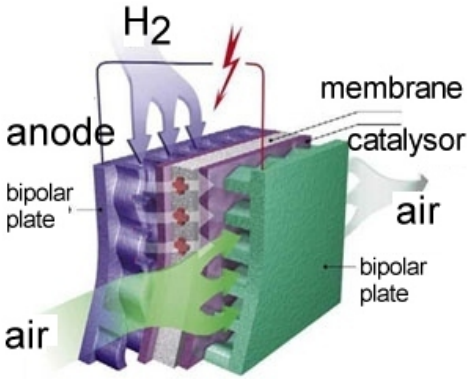

Figure 1. We show the principle of a fuel cell. Hydrogen and oxygen are fueled into different layers. They react, creating a potential which drives electric currents through the wires.

is inserted. Air or oxygen, respectively, is fueled at the cathode (-). They are separated by a semi-permeable membrane for protons with some catalysor (for example platin). Protons of hydrogen move to cathode through the membrane. This creates a potential which then drives electrones through wire and power some motor or light. Hydrogen and oxygen react at cathode to water and heat. Usually fuel cells need some heating and cooling technology.

We consider some fuel cell or fuel cell stack, respectively, as it can be seen in Figure 2. For our practical application Ω will be a domain which is a union of several cuboids. These cuboids are built by the end plates of fuel cells and the different layers of the fuel cell. For the mathematical modelling of the problem we assume Ω to be a Lipschitz domain in $\mathbb{R}^3$, which includes the above cases. We will choose our coordinate system such that the endplates are parallel to the $x_1 - x_2$ plane, x_2 is pointing upwards, and the current flowing through the active area moves in x_3-direction.

As described above, the currents are generated by chemical processes in the cell. There are two wires attached to the endplates, which carry the current to some consumer, possibly a vehicle or some immobile system. From the setting we know the current outside of the cell and, in particular, we know the inflowing and outflowing current on the boundary of the domain Ω. This leads to the boundary condition

$$\nu \cdot j(y) = g, \quad y \in \partial\Omega \tag{1}$$

with some given function g on $\partial\Omega$. We will describe a macroscopic modell to calculate the currents in the cell in Section 2. Currents are calculated on the basis of Ohm's law and the static Maxwell equations when some effective conductivity σ is provided.

Let us now assume that we know the current distribution j in the domain $\Omega \subset \mathbb{R}^3$. We need to model the magnetic field from which we target to reconstruct the current density j. Magnetic fields H of currents j are calculated via the *Biot-Savart integral operator*, defined by

$$(Wj)(x) := \frac{1}{4\pi} \int_\Omega \frac{j(y) \times (x-y)}{|x-y|^3}\, dy, \quad x \in \mathbb{R}^3 \tag{2}$$

for $j \in L^2(\Omega)$. For details about this representation and its relation to Maxwell's equations we refer to [10]. The problem of magnetic tomography now reduces to solving the equation

$$Wj = H_{meas} \quad \text{on } \partial G, \tag{3}$$

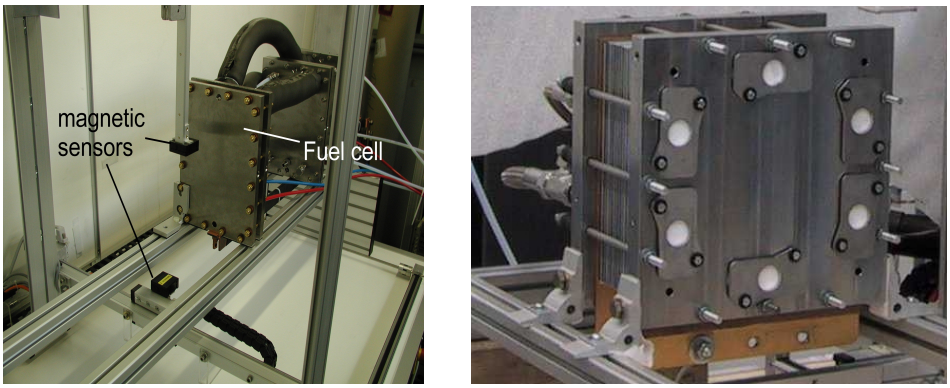

Figure 2. We show a fuel cell (left) and fuel cell stack (right) in the laboratory. The magnetic tomograph is seen in the left image with two magnetic sensors. With courtesy of TomoScience GbR, Wolfsburg / Research Center Jülich, Germany

where G is some domain with sufficiently smooth boundary such that $\overline{\Omega} \subset G$ and H_{meas} denotes some measured magnetic field on ∂G. Here, we need to supply appropriate conditions on the current densities j under consideration via the spaces on Ω and ∂G.

We will study the simulation of currents in Section 2. The uniquenss and non-uniqueness of current reconstructions is discussed in Section 3. Then, we present different approaches to current and obstacle reconstruction from measured magnetic fields in Section 4. In particular, we will describe a general *Tikhonov regularization approach* in Subsection 4.1, the *point source method* for field reconstructions in Subsection 4.2 and the *no-response test* in Subsection 4.3. Real data reconstructions will be provided in Section 5. We discuss some open problems at the end of each section.

2. Simulation of currents in fuel cells

The simulation of current densities in fuel cells is an important and difficult problem of current research in engineering. Via finite element tools a full community is involved in flow simulations within fuel cells.[1] However, so far it has not been possible to generate reliable and tested simulations which prove to reflect the real situation within the modern technological devices. One central problem here is the validation of models and calculations. The fuel cell is a quite sensitive and delicate technical system and it is difficult to measure inside the cell without changing the whole setting and with the setting the flow and currents in the cell.

Here, we will employ a macroscopic approach to the current simulation problem. We work with some macroscopic *effective* conductivity σ and impute *Ohms law* for the currents in the cell. Of course, this does not reflect the microscopic chemical and physical processes which are governing a typical fuel cell. But we incorporate key macroscopic physical laws which we believe to hold on a macroscopic scale in the cell and search for currents which satisfy these macroscopic laws.

First, we collect ingredients which have been used in [11]. For the electric and magnetic fields E and H we assume that the *static Maxwell field equations*

$$\begin{aligned} \operatorname{curl} H &= j, & \operatorname{curl} E &= 0 \\ \operatorname{div} D &= \rho, & \operatorname{div} B &= 0 \end{aligned} \tag{4}$$

[1] For example, the Company COMSOL based in Helsinki, Finland, develops the software FEMLAB for finite element simulations and, in particular, offers courses on the simulation of currents in fuel cells.

hold. Usually we will work in the case where there are no free charges, i.e. we have $\rho \equiv 0$. Further, we have the *material equations*

$$\begin{aligned} D &= \epsilon E, \qquad B = \mu H \\ j &= \sigma E \end{aligned} \tag{5}$$

with electric permittivity ϵ, magnetic suszeptibility μ, conductivity σ, elektric flux D and magnetic flux B. Equation (5) is known as *Ohm's law*. We assume that ϵ and μ are constant and equal to ϵ_0 and μ_0. Because of curl $E = 0$ there is an *electric potential* φ_E with $E = \nabla\varphi_E$. This potential is determined only up to a constant and we use a normalization condition to make it unique. Now, this yields $j = \sigma\nabla\varphi_E$. From

$$\text{div } j = \nabla \cdot \nabla \times H = 0 \tag{6}$$

and (5) we derive

$$\nabla \cdot \sigma\nabla\varphi_E = 0 \text{ in } \Omega. \tag{7}$$

We can now summarize the underlying problem in the following definition.

Definition 2.1 (Anisotropic Boundary Value Problem of Magnetic Tomography) *Consider a domain $\Omega \subset \mathbb{R}^3$ with Lipschitz boundary. Let σ be an* anisotropic conductivity *in Ω. We search for the electric potential φ_E such that the partial differential equation (7) is satisfied in Ω. This PDE is completed with the* boundary condition

$$\nu \cdot \sigma\nabla\varphi_E = g \tag{8}$$

on $\partial\Omega$ and the normalization

$$\int_\Omega \varphi_E(y)\, dy = 0. \tag{9}$$

From (6) we know that there are no currents generated in the domain Ω. Via the divergence theorem this leads to the *admissibility condition*

$$\int_\Omega \nabla \cdot j(y)\, dy \;=\; \int_{\partial\Omega} \nu(y) \cdot j(y)\, ds(y) \;=\; \int_{\partial\Omega} g(y)\, ds(y) \;=\; 0 \tag{10}$$

The solvability of the anisotropic boundary value problem Definition 2.1 has been investigated in [11]. The authors establish solvability of the problem in its weak form

$$\int_\Omega \nabla\psi \cdot \sigma\nabla\varphi_E dy = \int_{\partial\Omega} \psi\nu \cdot \sigma\nabla\varphi_E ds \tag{11}$$

for $\psi \in H^1(\Omega)$. We summarize the results in the following Theorem.

Theorem 2.2 (Uniqueness and Existence of Anisotropic Boundary Value Problem) *If the anisotropic conductivity distribution is* coerzitiv*, i.e.*

$$\Re\Big(v \cdot \overline{\sigma(y)v}\Big) \geq \gamma|v|^2,\ v \in \mathbb{R}^3,\ \ y \in \Omega \tag{12}$$

with some constant γ, then the problem given by Definition 2.1 has a unique weak solution in $H^1(\Omega)$ for all admissible boundary data g. The solution depends continuously on the boundary data as elements in $H^{-1/2}(\partial\Omega)$.

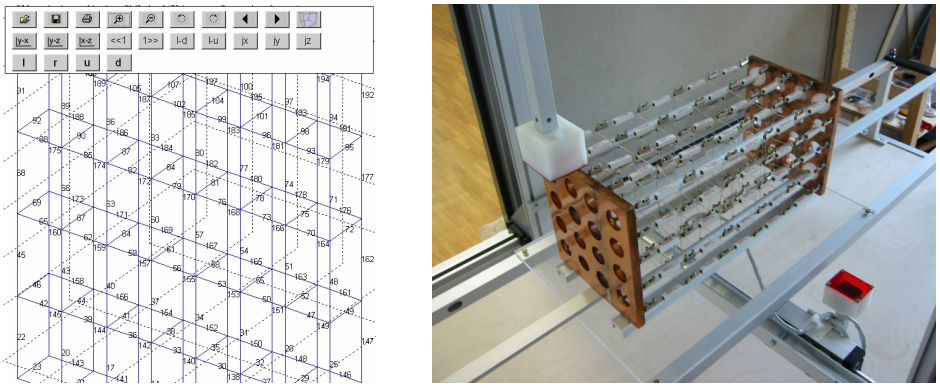

Figure 3. The grid for numerical computation of some single fuel cell and its physical simulation for a full stack of fuel cells via a wire grid (right). The above simple wire grid has been used for the first tests of magnetic tomography in 2002/03.

In [11] the authors employ the *finite integration technique* (FIT) for the numerical solution of the above boundary value problem. The finite integration technique uses the Maxwell equation in integral form on some cartesian grid. This is particular suitable for our situation, in which the domain Ω is a union of several cuboids. Here the finite integration technique can be realized by exactly calculating the currents flowing through some wire grid when the conductivities in the different wires are known. Wire grids can be realized physically, compare Figure 3, such that we solve a simplified real physical problem which has be used to test the algorithms of magnetic tomography.[2] The calculation of currents in a wire grid is carried out via *mesh* and *know rules*, also known as *Kirchhoff laws*.

THEOREM 2.3 (CONVERGENCE OF FIT) *Let σ be a coercive matrix. Then the equation system arising from mesh and knot rules has a* unique solution *for each discretization (n_1, n_2, n_3). For $n_j \to \infty$, $j = 1, 2, 3$, it* converges *towards the true solution of the boundary value problem.*

Here, convergence is understood in the sense that the discretized problem is extended into the space via some interpolation space. Kühn and Potthast [11] provide numerical examples in three dimensions.[3]

Open problems. *1. More complex wire grids.* Currently, the simulation of currents has been carried out on fairly easy grids to approximate the active area of a fuel cell. More elaborate grids need to be chosen and tested. As an error function we might use the simulated and measured magnetic field when the current densities are provided via some reference technology in the active layer of the cell. Such tests have been carried out, but only in a very preliminary stage.

2. Alternative numerical schemes. Investigate whether the finite integration technique provides the most appropriate and efficient scheme to simulate currents in a fuel cell. With the grid described above we work with currents which are focused in the wire grid. Higher-approximation methods for current simulation might prove to be more adequate and stable for current reconstruction when combined with appropriate projection schemes for discretization. We think that it is an important task to formulate and test different methods like the

[2] Compare Technical Reports of Tomoscience, some of which may be inaccessible due to confidentiality of the commercial product.

[3] The commercial Software MagneTom 4.0 of TomoScience is based on the finite integration technique and has been the basis for all results which we provide below.

finite element method, the *Nyström method* with higher order numerical quadrature and finite difference schemes.

3. Fast simulation methods. Currently the number of unknowns used for current simulation and fiel calculation is limited due to the fact that the mapping of the current into the magnetic field on ∂G has a complexity of $O(N \cdot K)$ for a dimension N of the space of currents and K evaluation points for H. It is highly desirable to develop fast simulation method, based either on the *fast Fourier transform* (FFT) or on approximation methods like H-matrices, the fast multipole-method or panel clustering. The FFT might bring the complexity down to $6O(N)$.

3. Uniqueness results

An important problem for magnetic tomography is given by the uniqueness question. Does a magnetic field measured on ∂G determine the current distribution in Ω? This question naturally leads to basic subproblems. *First*, do the measurements on ∂G determine the analytic magnetic field in the exterior of Ω? *Second*, if the field is determined on Ω_e, does it uniquely determine the current distribution j in Ω. We will first give a simple example which demonstrates the strong non-uniqueness of the general magnetic tomography problem.

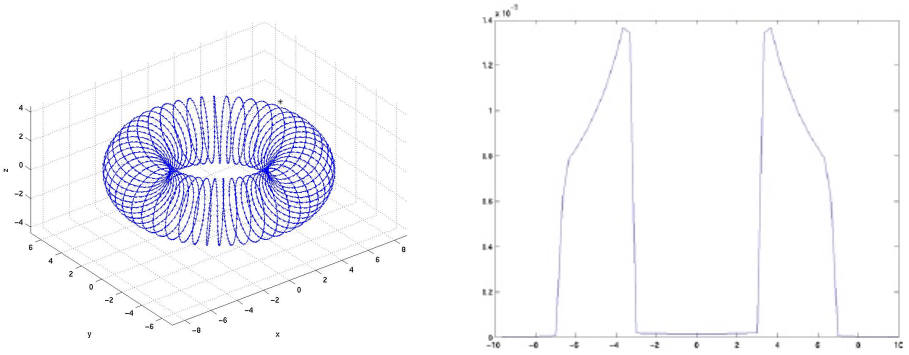

Figure 4. We show an element of the nullspace of the Biot-Savart integral operator. The right images shows the magnetic field on a line crossing the torus structure shown in the left image. The magnetic field is close to zero outside and strong in the interior of the torus.

Consider a vectorial function $m \in C_0^2(\Omega)$ and define $j := \triangle m$. We calculate

$$\begin{aligned}(Wj)(x) &= \operatorname{curl} \int_\Omega \frac{1}{4\pi}\frac{1}{|x-y|}\triangle m(y)dy \\ &= \operatorname{curl} \int_\Omega \triangle_y \frac{1}{4\pi}\frac{1}{|x-y|} m(y)dy \\ &= 0, \quad x \notin \overline{\Omega} \end{aligned} \tag{13}$$

where we used Green's second theorem and $\triangle_y \frac{1}{|x-y|} = 0$ for $y \neq x$. The full nullspace is characterized via the following result [5].

THEOREM 3.1 *The nullspace of the Biot-Savart integral operator (2) is given by the set*

$$N(W) = \left\{ \operatorname{curl} v : \ v \in H_0^1(\Omega), \operatorname{div} v = 0 \right\}. \tag{14}$$

Thus there is a large nullspace. Special elements of the nullspace have been constructed in [5], compare Figure 4. However, as soon as we pass to discrete wire grids, a general uniqueness theorem can be shown, which is due to the fact that the magnetic field $H(x)$ generated by a wire line γ with non-vanishing current has a singularity for $x \to \gamma$. Similar principles can be exploited to prove uniqueness for the current reconstruction from single-cells [18].

Connected to the uniqueness question is the characterization of the orthogonal space $N(W)^\perp$ of the nullspace $N(W)$ with respect to the $L^2(\Omega)$ scalar product

$$(\varphi, \psi)_{L^2(\Omega)} = \int_\Omega \overline{\varphi(y)}\psi(y)\, dy. \tag{15}$$

The space $N(W)^\perp$ is particularly interesting since the standard Tikhonov regularization (see Section 4.1) projects the solution density j onto the space $N(W)^\perp$. The following theorem is due to Kühn [9], extending results of [5].

THEOREM 3.2 *The* orthogonal space *of* $N(W)$ *is characterized by*

$$N(W)^\perp = \left\{ j \in H_{\mathrm{div}\,=0}(\Omega) : \ \exists q \in L^2(\Omega) \ s.d. \ \ \mathrm{curl}\, j = \mathrm{grad}\, q \right\}, \tag{16}$$

where $H_{\mathrm{div}\,=0}(\Omega)$ *denotes the set of densities* j *in* H^1 *with* $\mathrm{div}\, j = 0$.

An important *conclusion* of this result now follows from $\mathrm{div}\, j = 0$ via $\mathrm{curl}\,\mathrm{curl} = -\triangle + \mathrm{grad}\,\mathrm{div}$. We derive

$$\triangle j = -\mathrm{curl}\,\mathrm{curl}\, j = -\mathrm{curl}\,\mathrm{grad}\, q = 0 \tag{17}$$

for each element of $N(W)^\perp$. Equation (17) is to be understood in $H^{-1}(\Omega)$. Thus the cartesian components of the current density j are weak solutions to Laplace's equation and via standard regularity results they are also a strong solution to Laplaces equation. As it is well known (c.f. [8]) solutions of the Laplace equation satisfy a maximum-minimum principle, i.e. these functions take their maximum or minimum on the boundary of a domain. This is a strong limitation to the reconstruction algorithm via Tikhonov regularization which needs to be discussed further.

In Section 2 we have developed a boundary value problem for the simulation of currents in the cell. We call such currents *realistic* in the sense that they satisfy the underlying mathematical problem. What can we say about the reconstruction of realistic currents? Can such currents be uniquely determined from measurements of their magnetic fields. A partial answer is given by the following result [9, 5].

THEOREM 3.3 (RECONSTRUCTION OF REALISTIC CURRENTS) *Let* j *be a solution to the boundary value problem given by Definition 2.1. Then we have*

$$j \perp_\sigma N(W) \tag{18}$$

with orthogonality with respect to the scalar product

$$(\varphi, \psi)_\sigma := \int_\Omega \varphi(y) \cdot \sigma(y)^{-1} \overline{\psi(y)} dy. \tag{19}$$

The theorem shows that if σ is known, then the currents are in exactly the right space for unique reconstruction. However, if σ would be known we could calculate the currents by solving the forward problem and would not need the magnetic field measurements. Usually σ is unknown, that is the crucial point. In this sense the result of Theorem 3.3 does not help to answer the uniqueness question nor does it provide an algorithm for the reconstruction. However,

if σ is close to an homogeneous function, then the scalar product is close to the standard L^2 scalar product and we can employ an approximation argument. In this case we conclude that Tikhonov regularization will calculate a reasonable reconstruction by projecting onto the space $N(W)^{\perp}$ instead of the close space $N(W)^{\perp_\sigma}$.

Open problems. *1. Uniqueness for special situations.* It has been shown for some special situations that unique reconstruction of currents can be possible. For example, this result has been established for wire grids and a corresponding result for single-cells with continuous current distributions is possible [18]. Find further settings in which uniqueness can be shown.

2. Uniqueness for subspaces. Usually, for practical applications the problem of full continuous current reconstruction is far to difficult. The goal is to achieve reliable reconstructions of currents which are in some finite dimensional subspace X_n with sufficient spatial resolution (compare Section 4) in the $x_1 - x_2$ plane, i.e. over the active area of the cell. Develop a mathematical theory for uniqueness/non-uniqueness and stability for these situations.

4. Reconstruction of current densities and inclusions in fuel cells

The Biot-Savart operator (2) is a linear and bounded operator from $(L^2(\Omega))^3$ into $(L^2(\partial G))^3$. Moreover, since it has analytic kernel it is a compact operator. Due to the standard theory of compact linear operators they cannot have a bounded inverse and that equations of the form (3) are highly instable. Small perturbations in the data usually lead to strong perturbations in the reconstructions, such that naive inversion will not generate usefull results.

Over several decades many different *regularization methods* have been introduced to overcome the problem of instability for such operators [4]. The key idea is to replace the unbounded inverse W^{-1} by some bounded operator R_α depending on a *regularization operator* α. Here, we will focus on *three* different methods for reconstruction and outline their main ideas and results.

4.1. Reconstruction methods via Tikhonov regularization and projection schemes

A standard regularization technique is given by the *Tikhonov regularization* with

$$R_\alpha := (\alpha I + W^*W)^{-1}W^*, \quad \alpha > 0. \tag{20}$$

Calculating $j_\alpha := R_\alpha H$ is equivalent to minimizing the functional

$$\mu(j) := ||Wj - H||_{(L^2(\partial G))^3} + \alpha||j||_{(L^2(\Omega))^3}, \tag{21}$$

see [8]. It is shown in [4, 2] that the operator $R_\alpha : L^2(\partial G) \to L^2(\Omega)$ is bounded and that

$$R_\alpha H \to Pj, \quad \alpha \to 0, \tag{22}$$

where P denotes the orthogonal projection operator onto $N(W)^{\perp}$ in $(L^2(\Omega))^3$. The convergence (22) is *pointwise*, but not uniform. In particular, for every set of measurements H_{meas} with *data error* of size $||H_{meas} - Wj_{true}|| = \delta > 0$ we need to choose the regularization parameter α appropriately. Several methods for the *choice of* α for the operators of magnetic tomography based on stochastical principles are investigated in [1]. We remark that these methodds work well as long as the noise is mainly stochastic in nature. For noise arising from systematic measurement errors, most stochastic methods underestimate the noise and by choosing the regularization parameter too small they provide useless reconstructions which are polluted by artefacts.

The general application of the Tikhonov regularization to the magnetic tomography problem has advantages and disadvantages. First, it does not need to know further conditions like the boundary condition (8), the divergence condition (6) or *directional constraints*

$$e_3 \cdot j(y) \geq 0, \quad y \in \Omega, \tag{23}$$

which hold due to the chemical pathways of protons and electrons within the cell. This gives a large flexibility and guarantees the equation to remain linear. However, it also leads to a large number of unknowns. Since the number of unknowns are proportional to the ill-posedness of the equation, the use of general Tikhonov regularization will result in a more unstable system than equations which incorporate further constraints and conditions.

The following *projection method* provides the possiblity to flexibly incorporate conditions and knowledge about the unknown currents j. Let X_n be a subspace of dimension $n \in \mathbb{N}$ of our solution space $(L^2(\Omega))^3$. Here we assume that the functions $j \in X_n$ satisfy a set of constraints which we believe to hold for the current densities under consideration. Consider some basis $\left\{j^{(k)} : k = 1, ..., n\right\}$ of X_n. Then every element $j \in X_n$ can be written in terms of the basis functions

$$j = \sum_{k=1}^{n} \beta_k j^{(k)}. \tag{24}$$

By P we denote the orthogonal projection onto X_n. In this basis the Biot-Savart integral equation can be written as

$$\mathbf{W}\beta = QH \tag{25}$$

where Q is the orthogonal projection operator onto $Y_n := WX_n$, $\beta = (\beta_1, ..., \beta_k)^T$ and $\mathbf{W} = QWP$. We tested a Tikhonov method with regularization parameter α applied to the *projection equation* (25).

We have tested several spaces X_n, for example the divergence condition (6) in the form of Kirchhoff or knot rules, respectively, which leads to what we call *divergence free reconstruction*. In particular, for reconstructions from single cells where the only unknown is the conductivity component $\sigma_{33}(y)$ of the matrix $\sigma(y)$ for currents flowing through the membrane, we have chosen a *special basis* approach. In this case X_n is the space of simulated current densities which arise from particular choices of $\sigma_{33}(y)$, for details we refer to [7]. Results arising from real data will be shown in Section 5.

A *stochastic setting* for magnetic tomography for fuel cells has been investigated in [17]. In particular, the authors calculate the spatial distribution of the standard deviation in the $x_1 - x_2$ plane for a single cell. To this end three alternative methods are presented. The magnetic tomography problem is solved via a Markov Chain Monte Carlo Method with Gibbs sampler within the Bayesian approach.

4.2. The point source method

In this and the following section we will investigate a particular case of the magnetic tomography problem. We will assume that the conductivity σ is constant in $\Omega \setminus D$ with some domain $D \subset \Omega$ and constant in D. This is the case where some inclusion D with a conductivity different from the background conductivity is to be recovered.

As a preparation for the following reasoning as in [9] we rewrite the Biot-Savart representation of the magnetic field as

$$\begin{aligned} H(x) &= \operatorname{curl} \int_{\Omega\setminus D} \Phi(x,y) j(y) dy + \operatorname{curl} \int_D \Phi(x,y) j(y) dy \\ &= (\sigma_\Omega - \sigma_D) S_D(\nu \times E) + \sigma_\Omega S_\Omega(\nu \times E) \end{aligned} \tag{26}$$

with the *single-layer potential*

$$(S_G a)(x) = \int_{\partial G} \Phi(x,y) a(y) ds(y), \quad x \in \mathbb{R}^m. \tag{27}$$

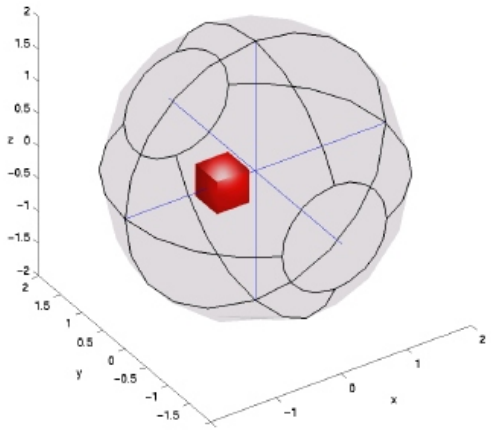

Figure 5. Setting for magnetic impedance tomography, where we try to find an inclusion in a homogeneous conducting material from measurements of the potential on the boundary $\partial\Omega$ of some domain Ω and the magnetic field H in the exterior of Ω for one single current density j.

Usually the exterior of Ω is an accessible region in space, thus it is reasonable to measure the potential φ_E on the boundary $\partial\Omega$. From this potential we can calculate the tangential components $\nu \times E$ of the static electric field. In contrast to the standard setting of impedance tomography (EIT) here we have these data available only for one fixed choice of the current density j.

The *point source method* provides a scheme how to evaluate the term

$$w(z) = S_D(\nu \times E)(z) = \int_{\partial D} \Phi(z,y)t(y)ds(y), \quad z \in \Omega \setminus D \tag{28}$$

with $t(y) = \nu(y) \times E(y)|_{\partial D}$ in magnetic impedance tomography from the knowledge of H. If in addition $\nu \times E$ on $\partial\Omega$ is known, we can calculate the magnetic field $H(x)$ in $\Omega \setminus D$. The full magnetic field in the interior is constructed by

$$H(z) \quad = \quad (\sigma_\Omega - \sigma_D)w(z) + \sigma_\Omega S_\Omega(\nu \times E)(z), \quad z \in \Omega \setminus \overline{D}. \tag{29}$$

We multiply $w(x)$, $x \in \partial\Omega$, by some vector field $a \in (L^2(\partial\Omega))^3$ and exchange the order of integration to derive

$$\begin{aligned} \int_{\partial\Omega} a(x)w(x)ds(x) &= \int_{\partial\Omega}\int_{\partial D} \Phi(x,y)t(y)ds(y)ds(x) \\ &= \int_{\partial D} \Big(\int_{\partial\Omega} \Phi(x,y)a(x)ds(x) \Big) t(y)ds(y) \\ &= \int_{\partial D} v(y)t(y)ds(y) \end{aligned}$$

where

$$v(y) := \int_{\partial\Omega} \Phi(y,x)a(x)ds(x), \quad y \in \Omega. \tag{30}$$

For the approximation $v(y) = v_z(y) \approx \Phi(y,z)$ we obtain

$$\mu[a] \quad := \quad \int_{\partial\Omega} a(x)w(x)ds(x)$$

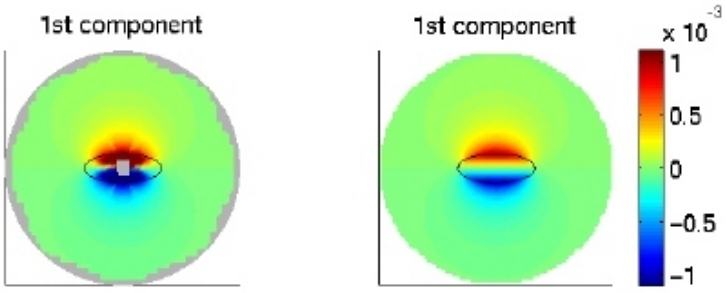

Figure 6. Reconstruction of some magnetic field arising from a current density with an elliptic inclusion in the center of our domain Ω. We show the first component $H_1(x)$ of the magnetic field simulated (right) and reconstructed (left). The reconstruction is valid only in the exterior of the inclusion, i.e. the fields in the interior of the inclusion do not have a meaning.

$$\begin{aligned} &\approx \int_{\partial D} \Phi(z,y)t(y)ds(y) \\ &= w(z) \end{aligned} \tag{31}$$

i.e. we approximately reconstruct the desired field.

Thus, the idea of the *point source method* is to approximate $\Phi(y,z)$ on some approximation domain G_z by a single-layer potential with density a_z living on $\partial\Omega$. Then $\mu[a_z]$ will approximate $w(z)$. The following theorem which proves the convergence of the point source method for magnetic field reconstruction in $\Omega \setminus \overline{D}$ is due to Kühn [9].

THEOREM 4.1 (CONVERGENCE OF POINT SOURCE METHOD) *Let a_n be a sequence of densities such that*

$$\Big|\Big|\Phi(\cdot,z) - \int_{\partial\Omega} \Phi(\cdot,y)a_n(y)ds(y)\Big|\Big|_{C(\partial D)} \to 0, \quad n \to \infty. \tag{32}$$

Then we have

$$(\sigma_\Omega - \sigma_D)\mu[a_n] + \sigma_\Omega S_\Omega(\nu \times E)(z) \to H(z), \quad n \to \infty. \tag{33}$$

for $z \in \Omega \setminus \overline{D}$

4.3. The no-response test

The point source method can process one set of data, it can reconstruct the magnetic fields, but it cannot locate the inclusion if the *boundary condition* is not known or if the boundary condition is a transmission condition. Thus, it is a basic problem to work on methods which can reconstruct the inclusion or its properties from measurements of the fields for *one* pair of data. One possible answer to this problem is the *no-response test*. We use a modification of the derivation (31) from above.

$$\begin{aligned} \mu[a] &= \int_{\partial\Omega} a(x) \underbrace{w(x)}_{=S_D(\nu\times E)(x)} ds(x) \\ &= \int_{\partial\Omega}\int_{\partial D} \Phi(x,y)t(y)ds(y)ds(x) \\ &= \int_{\partial D} \Big(\int_{\partial\Omega} \Phi(x,y)a(x)ds(x)\Big)t(y)ds(y) \end{aligned}$$

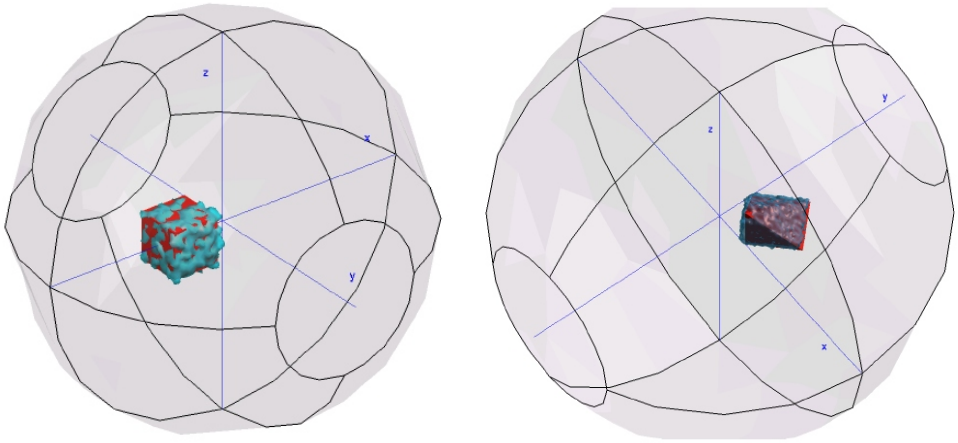

Figure 7. Reconstructions of some inclusion where the conductivity has been altered in some cuboid. The reconstruction via the no-response test uses magnetic field measurements and potential measurements for one current distribution.

$$= \int_{\partial D} v[a](y)t(y)ds(y)$$

where

$$v[a](y) := \int_{\partial\Omega} \Phi(y,x)a(x)ds(x), \quad y \in \Omega. \tag{34}$$

Here we now exploit the full freedom in the choice of the density a. The convergence of the no-response test for magnetic tomography is shown in [16].

THEOREM 4.2 (CONVERGENCE OF NO-RESPONSE TEST) *Let $\epsilon > 0$. The functional $\mu[a]$ with $a \in L^2(\partial\Omega)$ chosen such that*

$$||v[a]||_{C(\overline{G})} \leq \epsilon \tag{35}$$

is bounded if w is analytically extensible into $\Omega \setminus G$. If w is not analytically extensible into $\Omega \setminus \overline{G}$, then the supremum over $\mu[a]$ where a satisfies (35) is unbounded.

Here, analytic extension is understood in the sense that there is an analytic function in $\mathbb{R}^3 \setminus G$ which coincides with w on $\mathbb{R}^3 \setminus \Omega$. For a numerical realization of the no-response test we follow [9, 16].

DEFINITION 4.3 (NO-RESPONSE TEST) *We choose constants ϵ and C. Let $\mathcal{A}_\epsilon(G)$ be the set of densities $a \in L^2(\partial\Omega)$ such that*

$$||S_\Omega a||_{C(\overline{G})} \leq \epsilon. \tag{36}$$

The no response test calculates

$$\mu_\infty(G,\epsilon) := \sup_{a \in \mathcal{A}_\epsilon(G)} \mu[a] \tag{37}$$

and

$$D_{rec} := \bigcap_{\mu_\infty(G,\epsilon) \leq C} G \tag{38}$$

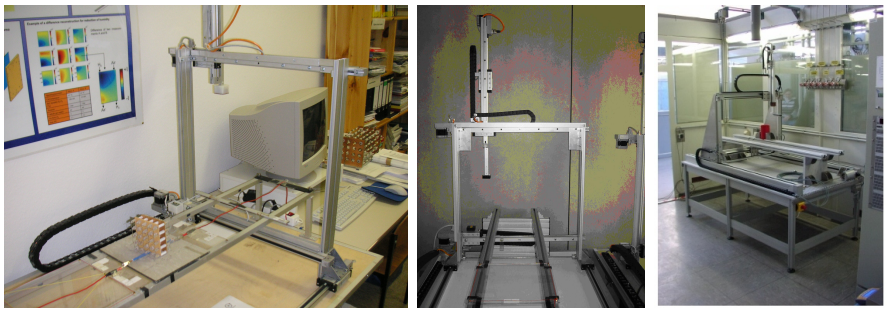

Figure 8. The images show the first, second and third prototype of the MagneTom measurement system for magnetic tomography. There are two sensors which can be moved independently around the cell to register the three-dimensional magnetic field.

Kühn has carried out numerical tests for the no-response test for magnetic tomography, compare Figure 7. For further details and reconstructions we refer to [9].

Open problems. *1. Choice of subspaces.* Develop a method for an optimal choice of the subspaces for magnetic tomography for fuel cells. The subspaces need to be sufficiently large to encorporate all possible currents. They need to use all conditions in a way such that measurement errors in the conditions (for example errors in the location of the boundaries of the cells) do not fully destroy the reconstructions. And the spaces have to be chosen such that they minimize the ill-posedness of the inverse problem under the above constraints.

5. Real data reconstructions and comparison with reference techniques

In this section we will discuss the realization of magnetic tomography in the measurement device *MagneTom* by TomoScience. A pilot paper for the full technology can be found in [6]. Magnetic measurements are carried out by *magnetic sensors* (C1), which in the easiest setup can be moved around by some mechanical hardware (C2) with electronic controls (C3). The system components for a magnetic tomography systems include control software (C4) for the mechanical parts and for the sensors (C5) as well as calibration software (C6). Further, to achieve adequate reconstructions there is a mathematical software component (C7) with simulation and reconstruction algorithms, which are controlled via some graphical user interface (C8). We remark that we needed extensive software development for the calibration process (C6) of the magnetic sensors, including simulation and optimization routines for sensor adjustments, which have turned out to be crucial steps as a preparation for the inversion schemes.

A machine to realize the steps C1 to C8 has been developed by TomoScience GbR Wolfsburg since 2001. Recently the third prototype has been a joint project with the Research Center Jülich, Germany[4]. The basic setup can be seen in Figure 8. The upper sensor can be moved freely in three dimensions, the movement of the lower sensor is bound to a plane in the $x_1 - x_3$ plane, where we choose x_3 to be along the long bars which can be clearly seen in each figure, x_2 vertically points to the top. As a *preprocessing step* we took measurements from a particular wire loop which was chosen to be of triangular form. In principle, this wire loop can be well simulated and we used the simulation and measurements to *calibrate* the exact location and orientation of the magnetic sensors on the chips in the sensor boxes, which can be seen in white or black, respectively, in Figure 8.

[4] Research Center Jülich, Institute for Materials and Processes in Energy Systems, Energy Process Engineering (IWV3), http://www.fz-juelich.de/iwv/iwv3/index.php

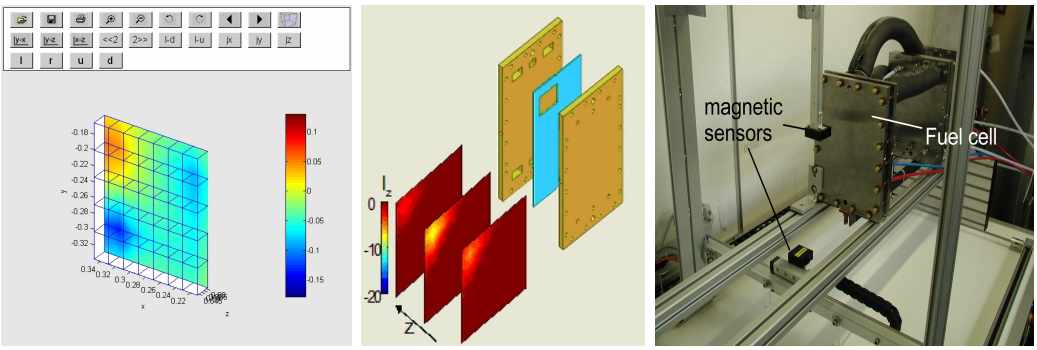

Figure 9. Detection of two holes in the membrane of the fuel cell, as indicated in the middle image. Left we show the reconstruction via magnetic tomography, the dark blue areas indicate regions of low current density. The right-hand image shows the fuel cell and the MagneTom machine.

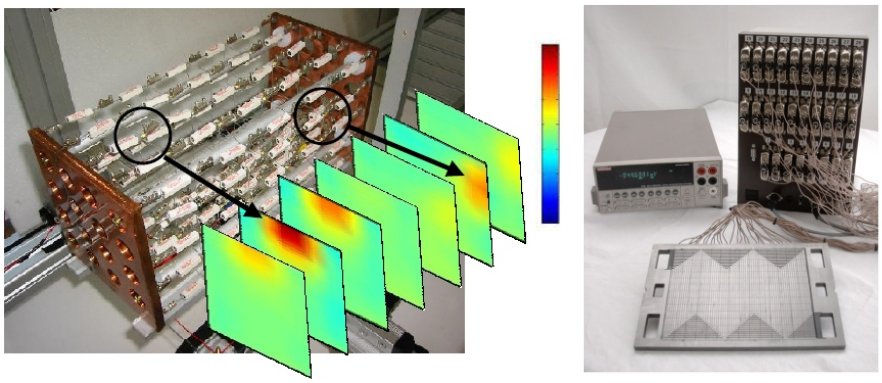

Figure 10. Reconstruction of currents in a three-dimensional wire grid from real-data measurements (left). The results show that in principle we can detect areas of low current density in a three-dimensional current distribution. The right-hand image shows the reference technology for the comparison displayed in Figure 11.

The basic principle for reconstructions for single-cells is shown in Figure 9. The currents are flowing through the active area of the fuel cell shown in the right-hand image. Here we have carried out reconstructions with two holes in the membrane which have been created artificially (see middle images) and lead to a reduction of the current density in the cell. These wholes can be clearly seen in the left-hand image of Figure 9, which is the three-dimensional representation of the currents in x_3-direction via a density plot. The blue grid lines in this image reflect the choice of the reconstruction grid on which via finite integration technique the currents and magnetic field have been calculated. The software allows free and interactive choice of all grid parameters via a graphical user interface. Further, the management of the dependencies of the different input parameters, data inputs and simulations on which the reconstruction is based has been carried out via a specially designed expert system.

For the real-data reconstructions we have employed the Tikhonov and projection methods described in Section 4.1. We found that the system includes strong systematic error into the measured magnetic field H. Therefore, to achieve good reconstructions we needed to work with a rather large regularization parameter α, usually between $\alpha = .5$ and $\alpha = 3$. We have

developed some *scaling method* to achieve a reliable scaling of the reconstructions. The scaling first calculates

$$j_{scal} := R_\alpha W j_0 \tag{39}$$

for some typical density j_0 and then determines a scaling constant via

$$c_\alpha := ||j_{scal}||_{L^2(\Omega)} / ||j_0||_{L^2(\Omega)}. \tag{40}$$

Finally, we correct the regularization scheme R_α by

$$j_\alpha := c_\alpha R_\alpha H_{meas}. \tag{41}$$

We call this the *scaled* Tikhonov or projection method.

Reconstructions from a threedimensional wire grid can be seen in Figure 10. This proves the feasibility of general three dimensional reconstructions, as they are targeted for general fuel cell stacks as shown in Figure 2. For a single-cell fuel cell based on hydrogen we show reconstructions in Figure 11. The results prove the feasibility of the method.

We remark that we have not managed to improve the reconstructions by using all the available information. In principle we can show by simulation that the reconstructions become more stable and reliable when the space X_n is chosen smaller [7]. However, so far for the real data in the fuel cell application the additional information seems to be polluted by measurement errors and it does not improve the outcome of the reconstruction procedure.

Figure 11 shows a comparison of the results of current reconstruction with magnetic tomography (right-hand column) and some reference technology [19] (left-hand column), where the currents are measured invasively by building wires into one of the layers and monitoring a potential gradient along this layer. The images have a common scaling, i.e. the each color in the pictures corresponds to the same current in mA/cm^2. This proves that the reconstruction of currents is in principle possible. The overall distribution of the current density is reconstructed. However, we think that the spatial distribution of the reconstructions needs to and can be improved.

Open problems. *1. Microscopic and macroscopic models.* Match the microscopic laws and models with the macroscopic laws and models to describe the processes and in particular the genesis and behaviour of currents in a fuel cell.

2. Error analysis. Develop models for the analysis of stochastic and - more important - systematic errors in magnetic tomography. Then, investigate both reconstruction methods and the choice of regularization parameters and create new methods for the optimal choice of regularization parameters in the presence of real-world noise.

3. Improved spatial resolution. Improve the spatial resolution of state-of-the-art magnetic tomography. This can be achieved for example by a reduction of the systematic error in a fuel cell, but it might also be possible to employ hierarchical methods for reconstruction, which reduce the ill-posedness of the full magnetic tomography problem.

4. Maximal potential of magnetic tomography. Evaluate the maximal potential of magnetic tomography by calculating what quality of reconstructions can be achieved with different error levels in the measurement of magnetic fields. This is of interest in particular in the practically relevant setting! Use stochastical methods for evaluating the error distributions.

5. Optimize the location of measurement points. Improve the results of magnetic tomography by optimizing the location of measurement points. We are free to choose the measurement points up to technical constraints given by the size of sensor boxes and the fuel cell end plates. Develop a technique to find measurement points which yield an optimal current reconstruction.

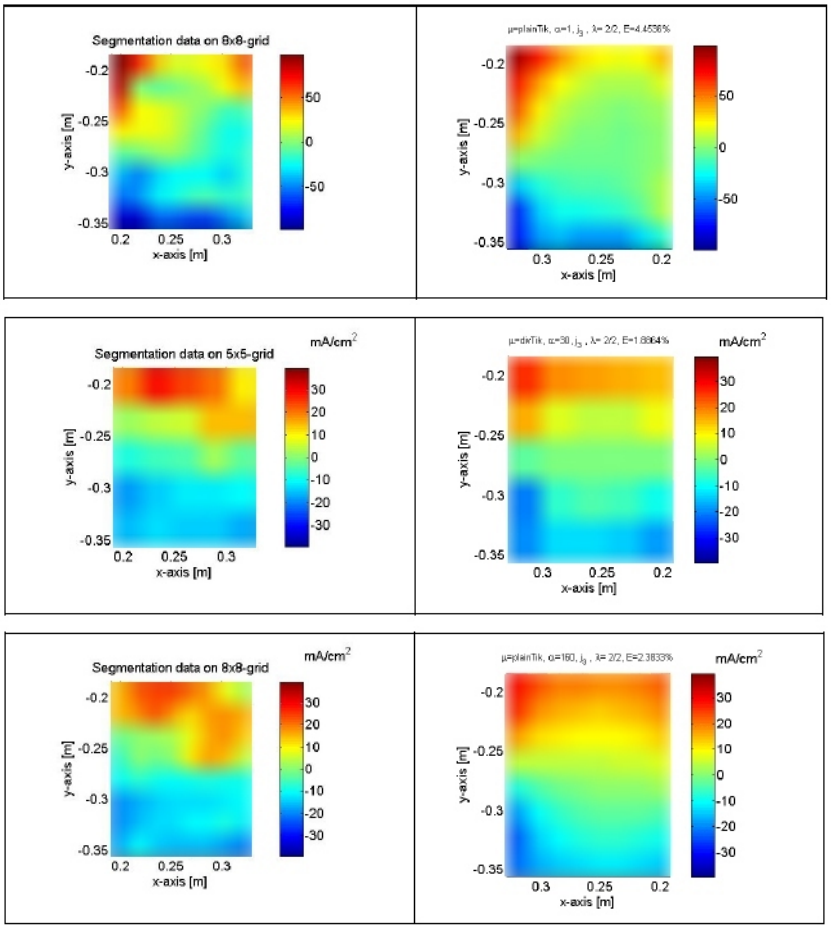

Figure 11. Comparison of the results of current reconstruction with magnetic tomography and some reference technology where the currents are measured invasively by building wires into one of the layers and monitoring a potential gradient along this layer. The images have a common scaling, i.e. the each color in the pictures corresponds to the same current in mA/cm^2. This proves that the reconstruction of currents is in principle possible. The overall distribution of the current density is reconstructed. However, the spatial distribution needs to be improved.

References

[1] Bauer F and Potthast R 2007 On the choice of the regularization parameter for magnetic tomography *Preprint*
[2] Colton D and Kress R 1998 *Inverse Acoustic and Electromagnetic Scattering Theory* (New York: Springer)
[3] Dohle H, Wannert M, Hauer K-H and Potthast R 2007 Magnetic Tomography for Direct Methanol Fuel Cell Technology *Preprint*
[4] Engl H-W, Hanke M and Neubauer A 1996 *Regularization of inverse problems* (Kluwer)
[5] Hauer K-H, Kühn L and Potthast R 2005 On uniqueness and non-uniqueness for current reconstruction from magnetic fields *Inverse Problems* **21** 1-13
[6] Hauer K-H, Potthast R, Stolton D and Wüster T 2005 Magnetotomography - A New Method for Analysing Fuel Cell Performance and Quality *Journal of Power Sources* **143** 67-74
[7] Hauer K-H, Potthast R and Wannert M 2007 Algorithms for magnetic tomography - on the role of apriori knowledge and constraints *Preprint*
[8] Kress R 1989 *Linear Integral Equations* (Springer)
[9] Kühn L 2005 Magnetic Tomography - On the Nullspace of the Biot-Savart Operator and Point Sources for Field and Domain Reconstruction. *Dissertation University of Göttingen*
[10] Kühn L, Kreß R and Potthast R 2002 The reconstruction of a current distribution from its magnetic fields.

Inverse Problems **18** 1127-1146
[11] Kühn L and Potthast R 2003 On the convergence of the finite integration technique for the anisotropic boundary value problem of magnetic tomography *Math. Meth. Appl. Sciences* **26** 739-757
[12] Kusiak S, Potthast R and Sylvester R 2003 A 'range test' for determining scatterers with unknown physical properties *Inverse Problems* **19** 533-547
[13] Potthast R 1998 A point-source method for inverse acoustic and electromagnetic obstacle scattering problems *IMA Journal of Appl. Math* **61** 119-140
[14] Potthast R 1996 A fast new method to solve inverse scattering problems *Inverse Problems* **12** 731-742
[15] Potthast R 2006 A survey about sampling and probe methods for inverse problems. *Topical Review* for *Inverse Problems* **22** R1-47
[16] Kühn L and Potthast R 2007 The point source method and the no-response test in magnetic impedance tomography *Preprint*
[17] Potthast R, Stratis I-G and Yannacopoulos A-N 2007 On the stochastic magnetic tomography problem *Preprint*
[18] Potthast R and Wannert M 2007 Uniqueness for magnetic tomography from a single-cell *Preprint*
[19] Wieser C, Helmbold A and Gülzow E 2000 A new technique for two-dimensional current distribution measurements in electrocemical cells *Journal of Applied Electrochemistry* **30** 803-807